THE ROYAL SOCIETY

Internal magnetic roughness in an iron–gadolinium multilayer

By H. Hashizume[1], S. Miya[1], T. Tanaka[1], N. Ishimatsu[1], Y. Yamaguchi[1], N. Hosoito[2], A. Sakuma[3] and G. Srajer[4]

[1]*Materials and Structure Laboratory, Tokyo Institute of Technology, Nagatsuta, Midori, Yokohama 226-8503, Japan*
[2]*Institute for Chemical Research, Kyoto University, Uji 611-0011, Japan*
[3]*Magnetic and Electronic Materials Research Laboratory, Hitachi Metals Ltd, Kumagaya 360-0843, Japan*
[4]*Advanced Photon Source, Argonne National Laboratory, Argonne, IL 60439, USA*

The q_z-dependent sign of the X-ray charge-magnetic interference diffuse scattering observed from an Fe–Gd multilayer is found to be due to rough internal magnetic interfaces in the Gd layers. The internal magnetic roughness is correlated with the charge roughness of the Fe–Gd interface. Born-approximation calculations using a fractal interface model show that the internal and Fe–Gd interfaces have similar magnetic roughness, as evidenced by the similar in-plane cut-off lengths of charge-magnetic height–height correlation functions.

Keywords: magnetic roughness; Fe–Gd multilayer; internal magnetic interface; charge-magnetic correlation length; X-ray diffuse scattering; resonant X-ray magnetic scattering

1. Introduction

Nelson *et al.* (1999) measured X-ray diffuse scattering from an $[\text{Fe–Gd}]_{15}$ multilayer at room temperature by switching the helicity of circular polarized photons of energy tuned close to the L_3 absorption edge of Gd, 7243.5 eV. The sample has a nominal structure of Si cap(3.5 nm)/$[\text{Fe}(3.5\ \text{nm})\text{Gd}(5.2\ \text{nm})]_{15}$, grown on a silicon (111) wafer in a vacuum-deposition chamber (10^{-6} Pa). The X-ray measurement was made on the SRI-CAT (Synchrotron Radiation Instrumentation Collaboration Access Team) 1-ID beamline at the Advanced Photon Source, Argonne National Laboratory, using a diamond quarter-wavelength phase plate, which converted the linear polarization of undulator light into a circular polarized beam. The 3.4 kOe in-plane field applied on the sample placed the $[\text{Fe–Gd}]_{15}$ multilayer in the so-called Fe-aligned state (Camley 1987; Camley & Tilley 1988) with the Fe and Gd magnetizations directed parallel and antiparallel to the applied field, respectively. All X-ray data were collected using the plane of scattering along the field direction. The energy resolution was *ca.* 1.5 eV. On the transverse q_x scans perpendicular to the specular rod at $q_x = 0$, the difference intensity, $I^+ - I^-$, decayed with a faster rate with increasing $|q_x|$ than the sum intensity, $I^+ + I^-$ (see fig. 2 of Nelson *et al.* (1999)). This indicates that the magnetic interfaces in the sample are smoother than the chemical (or charge) interfaces because $I^+ - I^-$ arises from the charge-magnetic interference scattering, whereas $I^+ + I^-$ is due to the pure charge scattering (Lovesey & Collins 1996). An ideally smooth surface without roughness produces no diffuse scatter and will show the fast decay of the specular reflection, which is determined by the angular profile of the probing beam. The $[\text{Fe–Gd}]_{15}$ data were fitted to an interface model of a self-affine fractal (Sinha *et al.* 1988) (figure 1), which shows roughness features with $\xi_e^{\parallel} = 200$ nm,† $\xi_e^{\perp} = 45$ nm and $h_e = 1.0$, where $\xi_e^{\parallel}$ and $\xi_e^{\perp}$ are the cut-off lengths of a charge-magnetic height–height correlation function in the in-plane and vertical directions, respectively, and h_e is the Hurst parameter. The simultaneously measured sum profiles, $I^+ + I^-$, indicate $\xi_e^{\parallel} = 50$ nm, $\xi_e^{\perp} = 45$ nm and $h_e = 0.32$ for the charge interface. The charge-magnetic roughness has a longer in-plane correlation length than the charge roughness, indicating a 'smoother' magnetic interface than the chemical interface. The off-specular scan shows clear Bragg-like peaks of similar widths in $I^+ - I^-$ and $I^+ + I^-$ (see fig. 1 of Nelson *et al.* (1999)), which encouraged the authors to assume the equal value quoted for $\xi_e^{\perp}$ and $\xi_e^{\perp}$. The root-mean-square charge and charge-magnetic roughness, σ_e, σ_e, was $0.8 \sim 1.2$ nm. These values compare well with those reported by Freeland *et al.* (1998) for Cu/CoFe/Cu sandwiches. The results, indicating the distinct roughness properties of chemical and magnetic interfaces, are in qualitative agreement with the earlier work by MacKay *et al.* (1996).

A striking feature of figure 1 is that $I^+ - I^- > 0$ at $q_z = 1.41$ nm^{-1} and $I^+ - I^- < 0$ at $q_z = 2.12$ nm^{-1}, which are the q_z values of the second and the third multilayer Bragg peaks on the specular rod, respectively. As discussed in Nelson *et al.* (1999), the sign reversal of the diffuse peaks cannot be accounted for so long as we assume uniformly magnetized Gd layers. The curve for $q_z = 2.12$ nm^{-1} in figure 1, calculated for a uniform magnetization, only fits the observation when inverted in sign (dotted line). The fit has a problem in this sense. The Fe magnetization does not concern us here. Non-resonant magnetic scattering from Fe atoms is very much weaker than the resonance-enhanced Gd scattering.

In fact, each Gd layer magnetizes highly non-uniformly along the out-of-plane direction (figure 2). Interface sublayers nearly fully magnetize, whereas the interior sublayers are free from magnetization. The localized magnetizations in the paramagnetic Gd layer are induced by the magnetized Fe layers through the Fe–Gd antiferromagnetic interaction. Gd moments are more aligned antiparallel to the applied in-plane field in the interface regions than in deeper sublayers. The map in figure 2 is derived from an analysis of charge-magnetic specular reflections measured at the Gd L_3 edge, assuming chemically uniform layers with abrupt smooth interfaces. This map explains quite well the positive and negative interference Bragg peaks observed at $q_z = 1.41$ and 2.12 nm^{-1} on the specular rod, respectively.‡ Both specular and diffuse components of $I^+ - I^-$ are thus positive at $q_z \sim 1.41$ nm^{-1} and negative at $q_z \sim 2.12$ nm^{-1}. In other words, the charge scattering and the magnetic scattering are in phase at $q_z \sim 1.41$ nm^{-1} and 180° out of phase at $q_z \sim 2.12$ nm^{-1}. The postulated chemical uniformity is supported by a fit to sum signal $I^+ + I^-$: the specular

† We quoted $\xi_e^{\parallel} = 152$ nm in Nelson *et al.* (1999). This value was obtained using a model of Si cap(2.0 nm)/Fe silicide(2.0 nm)/Fe(3.6 nm)[Gd(5.3 nm)/Fe(3.6 nm)]$_{14}$Gd(5.3 nm)/Si substrate for the multilayer structure. We use in this paper a simpler model of Si cap(3.5 nm)/[Fe(3.48 nm)/Gd(5.43 nm)]$_{15}$/Si substrate, refined by a fit to the charge-specular reflectivity profile.

‡ The sign of $I^+ - I^-$ sensitively depends on the exact X-ray energy near the absorption edge. The described observations were made at 7243.5 eV, where the real part of the resonant magnetic scattering form factor of Gd, f'_m is negative. All peak signs are reversed at 7247.5 eV, where $f'_m > 0$ (Ishimatsu *et al.* 1999). Discussions in the text refer to 7243.5 eV.

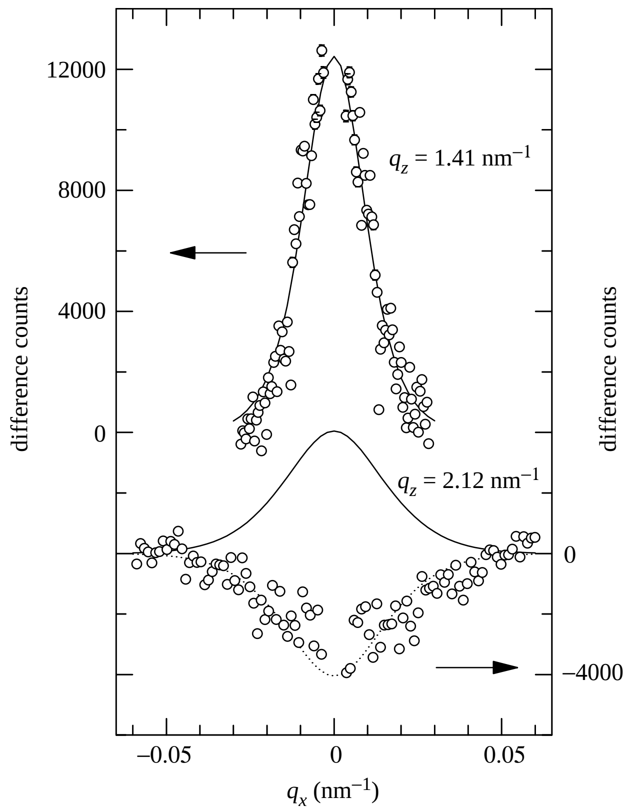

Figure 1. Resonant X-ray magnetic-charge interference diffuse scattering from the $[\text{Fe–Gd}]_{15}$ multilayer at room temperature. The data were collected in 83 h. The specular peaks are eliminated in the $q_x \sim 0$ region. Solid lines show Born-approximation fits using a fractal Fe–Gd interface model. The dotted line shows a mirror image of the fit at $q_z = 2.12\ \text{nm}^{-1}$. Fitting parameters: $\sigma_\text{e} = 1.2$ nm; $\xi_\text{e}^{\parallel} = 200$ nm; $\xi_\text{e}^{\perp} = 45$ nm; $h_\text{e} = 1.0$.

and off-specular profiles are reasonably well fit by a model assuming uniform electron densities in the Gd and Fe layers with rough interfaces between them.

In what follows, we will show that each Gd layer contains internal rough magnetic interfaces and that these are responsible for the sign-reversed charge-magnetic interference diffuse peaks. Readers unfamiliar with X-ray magnetic scattering are encouraged to refer to the excellent monograph by Lovesey & Collins (1996).

2. Internal magnetic interfaces

The map in figure 2 indicates magnetic interfaces between sublayers of distinct local magnetizations in the chemically uniform Gd layer. These are called internal magnetic interfaces, as opposed to the external interfaces located at the Fe–Gd boundaries. Charge scattering, specular and diffuse, occurs at the rough Fe–Gd interfaces (figure 3*a*). We ignore here the cap layer and the substrate. Scattering by domain walls and small defects is also neglected. If an internal magnetic interface is smooth with no roughness, only resonant magnetic specular reflection can take place on this interface, with no diffuse beam produced (figure 3*b*). The magnetic specular beams

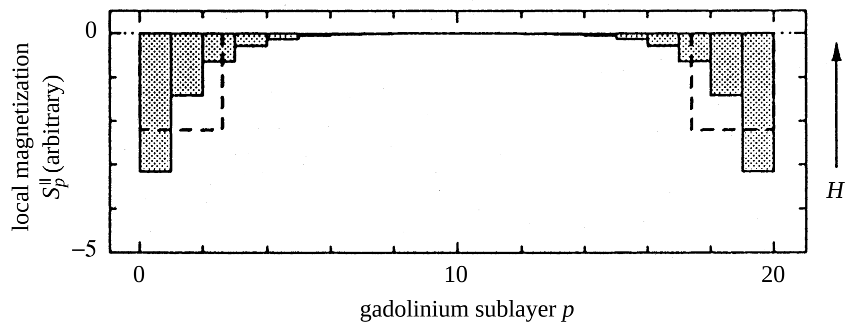

Figure 2. Magnetization profile for the Gd layers in a $[Fe–Gd]_{15}$ multilayer at room temperature, determined from the X-ray specular reflection data (Ishimatsu *et al*. 1999). A Gd layer is divided into 20 sublayers, for which the parallel magnetization components are shown by histograms. The Fe–Gd interfaces are located at $p = 0$ and 20. H indicates the direction of the applied in-plane field. The broken line shows a simplified square profile used in a later section of this paper.

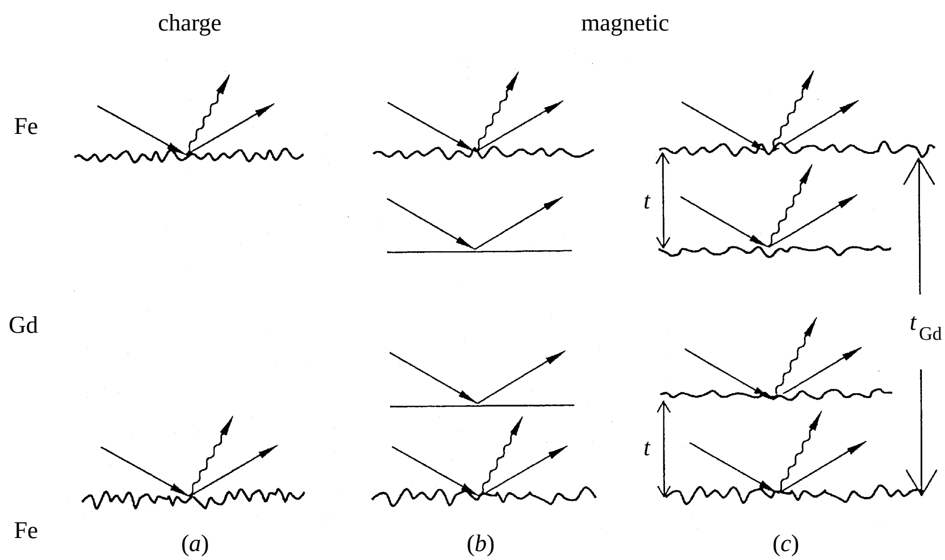

Figure 3. Resonant charge (a) and magnetic (b), (c) scattering in the Fe–Gd multilayer. The charge scattering, specular (straight line) and diffuse (wavy line), occurs at the rough external interfaces of the chemically uniform Gd layers. The magnetic scattering takes place at the external and internal magnetic interfaces, but the diffuse beams are only produced on rough interfaces.

from individual interfaces, internal and external, interfere with each other and with the charge-specular beams from the Fe–Gd interfaces to give rise to a sharp positive interference Bragg peak at $q_z = 1.41\ \mathrm{nm}^{-1}$ and a negative peak at $q_z = 2.12\ \mathrm{nm}^{-1}$ (Ishimatsu *et al*. 1999). The phase of magnetic scattering from each electron is shifted by the resonance effect so that it interferes with the charge scattering. The magnetic specular beam from an interface may be diffusely scattered on reaching an Fe–Gd interface, which is magnetically rough. This is a weak secondary effect, however, and only the primary diffuse scattering is considered in the Born approximation. For the

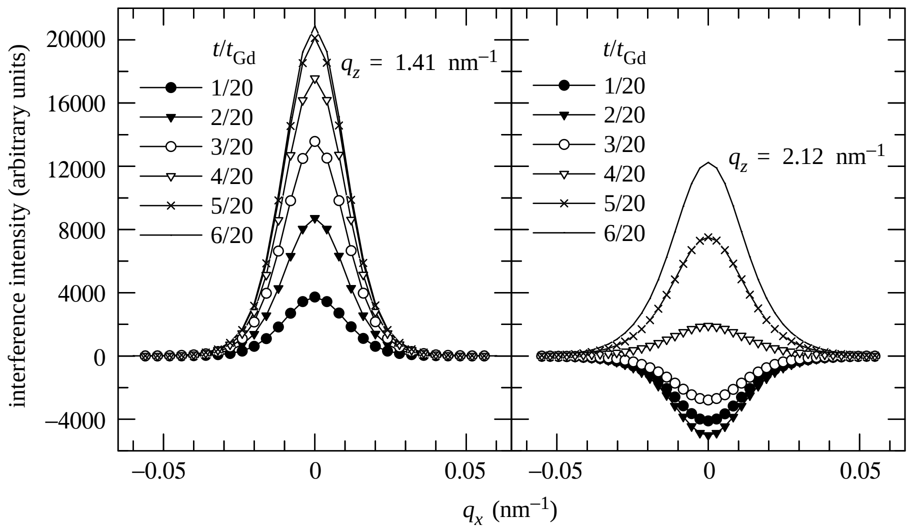

Figure 4. Interference diffuse profiles at $q_z = 1.41$ and $2.12\,\mathrm{nm}^{-1}$ for the [Fe–Gd]$_{15}$ multilayer. Each Gd layer of thickness t_{Gd} contains two rough internal magnetic interfaces at distance t from the Fe–Gd interfaces. The calculation assumes $\sigma_{\mathrm{e}} = 0.8$ nm, $\xi_{\mathrm{e}}^{\parallel} = 155$ nm, $\xi_{\mathrm{e}}^{\perp} = 45$ nm, $h_{\mathrm{e}} = 1.0$.

same reason, we ignore multiple charge scattering. Magnetic diffuse scattering only occurs at the Fe–Gd interfaces. In this case, the charge-magnetic interference diffuse intensity has a same sign at $q_z \sim 1.41$ and $2.12\,\mathrm{nm}^{-1}$, or at any q_z, like diffraction from a crystal of a single atom per unit cell, which is inconsistent with the observation. While the specular component of $I^+ - I^-$ is modulated in q_z by the interference between the external and internal interfaces, the diffuse component is not.

The difference diffuse intensity can have a q_z-dependent sign if the internal magnetic interfaces are rough. Both specular and diffuse beams of magnetic scattering are generated on each internal interface (figure 3*c*). If the internal magnetic roughness is correlated with the charge roughness at the external interfaces, the interference between the two diffuse beams will modulate the difference diffuse intensity as a function of q_z. Clearly, the specular and diffuse components of $I^+ - I^-$ have a common sign at an arbitrary q_z value. It is to be noted that the non-uniform Gd magnetization in itself does not explain the observed sign reversal of the interference diffuse intensity. The internal magnetic interfaces must be rough.

The argument is formulated as follows. The cross-section of charge-magnetic interference diffuse scattering from a multilayer is dictated by

$$\frac{1}{q_z^2}\sum_{j,k}\exp(-q_z^2\sigma_{\mathrm{e},jk}^2)\exp(-\mathrm{i}q_z(z_j - z_k))\int[\exp(q_z^2 C_{\mathrm{e},jk}(x)) - 1]\exp(-\mathrm{i}q_x x)\,\mathrm{d}x, \tag{2.1}$$

where $C_{\mathrm{e},jk}(x)$ is a function describing the charge-magnetic height–height correlation between charge interface j and magnetic interface k, located at $z = z_j$ and z_k, respectively. The y direction has been integrated by the wide slits used in the experiment. For fractal interface planes,

$$C_{\mathrm{e},jk}(x) = \sigma_{\mathrm{e},jk}^2\exp[-(x/\xi_{\mathrm{e},jk}^{\parallel})^{2h_{\mathrm{e},jk}}]\exp(-|z_j - z_k|/\xi_{\mathrm{e},jk}^{\perp}). \tag{2.2}$$

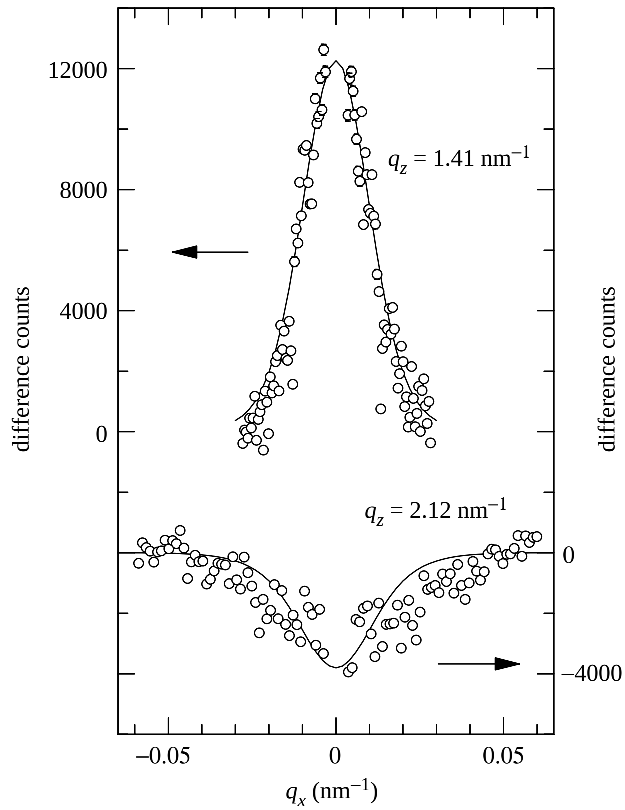

Figure 5. Fits using a square magnetization profile with internal interfaces at $t/t_{\mathrm{Gd}} = 0.134$ and 0.866 in the Gd layer. Fitting parameters: $\sigma_{\mathrm{e},jk} = 0.8$ nm; $\xi^{\parallel}_{\mathrm{e},jk} = 155$ nm; $\xi^{\perp}_{\mathrm{e},jk} = 45$ nm; $h_{\mathrm{e},jk} = 1.0$.

For the structure of figure 3*c*, $C_{\mathrm{e},jk}(x)$ with $j = k$ accounts for the in-plane charge-magnetic roughness correlation of an external interface, whereas $C_{\mathrm{e},jk}(x)$ with $j \neq k$ represents the correlation between the charge roughness of an external interface and the magnetic roughness of an internal interface or of a separate external interface. The theoretical curves in figure 1 only take $C_{\mathrm{e},jk}(x)$ for the external interfaces into account. In the following discussion, we fix $h_{\mathrm{e},jk} = 1.0$ and $\xi^{\perp}_{\mathrm{e},jk} = 45$ nm for all j and k (Nelson *et al*. 1999). The $h_{\mathrm{e},jk}$ value appears to be too large for a vacuum-deposited film, but it does not affect the discussion that follows.

For demonstration purposes, we simplify the magnetization profile in figure 2 to a square profile having two internal magnetic interfaces displaced from the Fe–Gd interfaces by t (see the broken line). The outer sublayers have a finite magnetization ($S^{\parallel}_{\mathrm{p}} = S$) and the central sublayer of thickness $t_{\mathrm{Gd}} - 2t$ is free from magnetization ($S^{\parallel}_{\mathrm{p}} = 0$). One can scale $S = 1$ to the saturation magnetization of bulk Gd, but, clearly, S works just as a scaling factor in the following calculations. We assign, for the time being, the same magnetic roughness to the external and internal interfaces, i.e. $\sigma_{\mathrm{e},jk} = 0.8$ nm and $\xi^{\parallel}_{\mathrm{e},jk} = 155$ nm for all j and k. Figure 4 shows calculated interference diffuse profiles, which are all positive at $q_z = 1.41\,\mathrm{nm}^{-1}$. At $q_z = 2.12\,\mathrm{nm}^{-1}$, the diffuse peak is negative for $t/t_{\mathrm{Gd}} < 0.18$ and changes

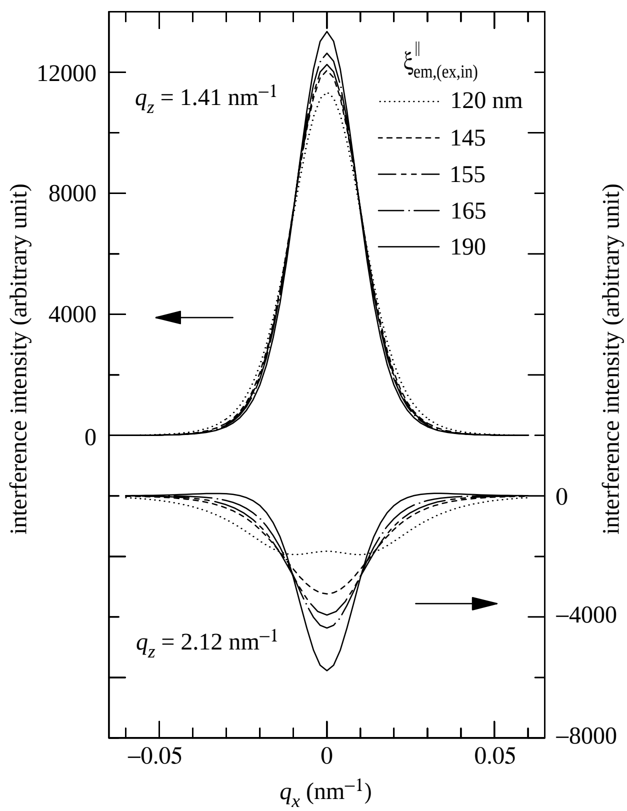

Figure 6. Effect of varied magnetic correlation lengths in the internal interfaces. Calculated using: $t/t_{\mathrm{Gd}} = 0.134$; $\sigma_{\mathrm{e},jk} = 0.8$ nm; $\xi^{\perp}_{\mathrm{e},jk} = 45$ nm; $h_{\mathrm{e},jk} = 1.0$ for all j and k; and $\xi^{\parallel}_{\mathrm{e(ex,ex)}} = 155$ nm.

sign at $t/t_{\mathrm{Gd}} \sim 0.18$. This shows that rough internal magnetic interfaces located close to the Fe–Gd interfaces play a crucial role in producing the sign-reversed diffuse peaks. The profile variation in figure 4 evidences the interference between the external and internal interfaces, which is controlled by t/t_{Gd}. The charge-magnetic specular Bragg peaks show the same t/t_{Gd} behaviour as the diffuse peaks, which is evident from the preceding argument, but was confirmed. In figure 1, the diffuse peaks at $q_z = 1.41$ and $2.12\,\mathrm{nm}^{-1}$ have a 1:0.32 height ratio. This is yielded by $t/t_{\mathrm{Gd}} = 2.67/20$ in our model (figure 5). The internal interfaces are located near the middles of the third histograms from the Fe–Gd interfaces in figure 2. If they sit deep in the zero-magnetization region in figure 2, the square model is known to be inappropriate.

3. Discussion

Figure 6 illustrates the effect of distinct magnetic roughness in the external and internal interfaces, which is studied by varying $\xi^{\parallel}_{\mathrm{e(ex,in)}}$ with $\xi^{\parallel}_{\mathrm{e(ex,ex)}}$ fixed at 155 nm. With increasing $\xi^{\parallel}_{\mathrm{e(ex,in)}}$, the interference diffuse intensity shows faster $|q_x|$ decay features, as expected, and the peak-height ratio increases. It is hard to decide on a best-fitting profile, but $\xi^{\parallel}_{\mathrm{e(ex,in)}} = 145$ nm appears to provide a slightly better

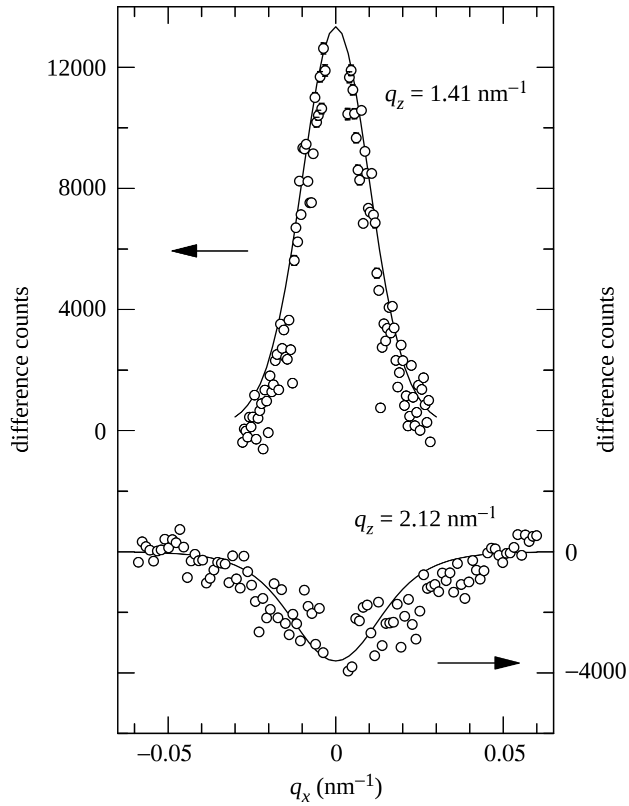

Figure 7. Fits using distinct magnetic roughness correlation lengths for the external and internal interfaces, $\xi^{\parallel}_{\mathrm{e(ex,ex)}} = 155$ nm and $\xi^{\parallel}_{\mathrm{e(ex,in)}} = 145$ nm. See the caption of figure 5 for the other parameters.

fit than 155 nm (figure 7). We can also relax the constraints on $\sigma_{\mathrm{e},jk}$ and $h_{\mathrm{e},jk}$ to explore the mean roughness amplitude and texture of the internal magnetic interface, but, clearly, high-quality data are required for further studies. A wider q_z coverage spanning the first and fourth Bragg peaks is desirable to reveal details. Much can be learned from simple models, but one can certainly make up a more realistic model of extended magnetic interface than the one used in this paper. Theoretical work has to be done in the future to isolate magnetic roughness by deconvoluting charge-magnetic roughness with known charge-roughness information. The magnetic roughness is a representation of magnetic disorder at the interface, which scatters spin-polarized electrons and strongly affects the magnetotransport in ferromagnetic tunnel junctions and giant magnetoresistance structures.

This work is supported by Monbusho Grant-in-Aids, contracts 0930519, 10044071 and 10130101 and by US DOE-BES under contract no. W31-109-ENG-38.

References

Camley, R. E. 1987 *Phys. Rev.* B **35**, 3608.

Camley, R. E. & Tilley, D. R. 1988 *Phys. Rev.* B **37**, 3413.

Freeland, J. W., Chakarian, V., Bussmann, K., Idzerda, Y. U., Wende, H. & Kao, C. C. 1998 *J. Appl. Phys.* **83**, 6290.

Ishimatsu, N., Hashizume, H., Hamada, S., Hosoito, N., Nelson, C. S., Venkataraman, C. T., Srajer, G. & Lang, J. C. 1999 *Phys. Rev.* B **60**. (In the press.)

Lovesey, S. W. & Collins, S. P. 1996 *X-ray scattering and absorption by magnetic materials*, ch. 6.1. Oxford Science.

MacKay, J. F., Teichert, C., Savage, D. E. & Lagally, M. G. 1996 *Phys. Rev. Lett.* **77**, 3925.

Nelson, C. S., Srajer, G., Lang, J. C., Venkataraman, C. T., Sinha, S. K., Hashizume, H., Ishimatsu, N. & Hosoito, N. 1999 *Phys. Rev.* B **60**. (In the press.)

Sinha, S. K., Sirota, E. B., Garoff, S. & Stanley, H. B. 1988 *Phys. Rev.* B **38**, 2297.